

TARGET DETECTION USING FORWARD SCATTERING RADAR WITH GPS RECEIVERS

Christo Kabakchiev

*Faculty of Mathematics & Informatics, Sofia University, 125 Tzarigradsko shose Blvd., Sofia, Bulgaria
ckabakchiev@fmi.uni-sofia.bg, ckabakchiev@yahoo.com*

Vera Behar

*Institute of Information & Communication Technologies, BAS, 25-A Acad. G.Bonchev Str., Sofia, Bulgaria
behar@bas.bg*

Herman Rohling

*Department of Telecommunications, TU hamburg-Harburg, Hamburg, Germany
rohlingr@tu-harburg.de*

Keywords: Forward scattering radar, target detection, GPS signal processing

Abstract: A possible algorithm for target detection in a GPS-based Forward Scattering Radar is considered. The FSR system consists of a transmitter mounted on a satellite of GPS and a receiver located on the Earth's surface. Theoretical calculations are presented using the secondary application of the GPS L5 signal. The numerical results illustrate the idea of target detection in GPS-based FSR.

1 INTRODUCTION

Forward Scattering Radar (FSR) is a specific type of bistatic radars that operate in the narrow area of the forward scattering effect where the bistatic angle is close to 180° , and the target moves near the transmitter-receiver baseline. In FSR the Babinet's principle is exploited to form the forward scatter signature of a target (Chernyak, 1999). According to this principle, the drastic enhancement in scattering is created due to the forward scattering effect. This type of radar provides a countermeasure to 'stealth' technology because due to the forward scattering effect, the Radar Cross Section (RCS) of targets extremely increases (by 2-3 orders) and mainly depends on the target's physical cross section and is independent of the target's surface shape and the absorbing coating on the surface. However, FSR has some fundamental limitations, which are the absence of range resolution and operation within very narrow angles ($\pm 10^\circ$) (Cherniakov et al., 2006).

In this paper a passive FSR system where the satellites of the GPS system are exploited as 'illuminators of opportunity' is considered. (Fig. 1). The civil L1 signal is transmitted by satellites at

1572.42 MHz and contains the coarse acquisition (C/A) code, which is unique for each satellite. The C/A code modulated signal is a BPSK signal with a chip rate of 1.023 MHz and the repetition interval of 1ms. The L1 signal frequency bandwidth is 2.046 MHz. The idea to apply a GPS L1 receiver to FSR for air target detection is firstly discussed in (Koch and Westphal, 1995). Some experimental results of a GPS L1 receiver concerning detection of air targets are shown and discussed in (Suberviola et al., 2012). However, modernization of GPS provides a good opportunity to use the improved properties of a new designed civil GPS signal L5 in FSR, which exploits GPS as a non-cooperative transmitter. The major innovations of the signal L5 signal, with respect to GPS L1 signal, are the additional NH code modulation and the use of a pilot channel free of data (Mongredien et al., 2006).

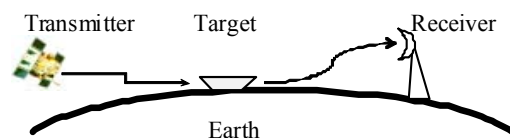


Figure 1. FSR topology

The L5 signal is transmitted at 1176.45 MHz with a received power of -154 dBw, which makes the L5 signal four times stronger than the L1 signal. Two quadrature components of the L5 signal, referred as I5 and Q5, are bi-phase modulated with a different PRN of length 10230 chips. The PRN codes are generated at a 10.23 MChips/s rate, resulting in 1 ms period. Therefore, the bandwidth of the L5 signal is increased to 20.46 MHz, which is ten times wider than the bandwidth of the L1 signal. The I5 and Q5 components are then modulated by a 10-bit NH-sequence and a 20-bit NH-sequence, respectively. Each bit of the NH-sequences is 1ms, resulting in 10ms period of the I5 component and 20ms period of the Q5 component, respectively.

A possible algorithm for air target detection in a GPS L5-based FSR system is described in (Behar and Kabakchiev, 2011), and the detection probability characteristics are calculated in (Behar et al., 2011) for the case when low-flying and poorly maneuverable (for example, helicopters) air targets are detected on the background of a white Gaussian noise, or in the presence of: Urban Interference Environment or a Stand-off-Jammer (SOJ).

Our main aim in this paper is to show perspectives of GPS-L5-based FSR systems to reliably detect ground or marine targets when GPS satellites are located at small elevation angles. Our task here is to present a possible algorithm for marine target detection and target parameter estimation in a GPS receiver used in FSR and also to roughly estimate the potential maximum target detection range in conditions of sea clutter. A set of experimental records of signals from a small boat provided by the team of Birmingham University is used in order to estimate Signal-to-clutter-plus-noise ratio (SNR) and calculate the probabilities characteristics.

2 SIGNAL PROCESSING

The general block-scheme of a possible algorithm for target detection and parameter estimation is shown in Fig.2.

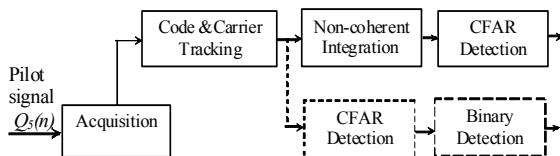


Figure 2. FSR signal processing

The Q5 component from the front end including filtering and down conversion is then sampled by the

A/D converter. The signal from satellite k after the A/D conversion can be described as

$$Q_5(n) = A(n)c_Q(n)NH_{20}(n)\cos(\omega_{IF}n) + N(n) \quad (1)$$

where n is discrete in time, ω_{IF} that is the intermediate frequency to which the front end has down converted the carrier frequency, $N(n)$ is the total noise, and $c_Q(n)$ is the PRN code. The main goal of acquisition is the roughly estimation of the Doppler frequency and the $(c_Q \cdot NH_{20})$ code delay of the visible satellite. The tracking loops ensure that the prompt correlator is synchronized with the incoming pseudorandom $(c_Q \cdot NH_{20})$ code. They also synchronize the receiver local oscillator in frequency and phase with each satellite signal carrier within the period of the Q5 component of the GPS L5 signal. In this manner, the correlation magnitude remains in the real part only (in-phase component). Two variants of algorithms can be used for target detection. The first of them firstly integrates signal within a moving window and then uses a CFAR detector to indicate the target signal detection (CFAR detection with non-coherent integration). According to the second algorithm, a CFAR detector firstly indicates whether the target signal is present in each sample of the correlator output. After that the binary detector indicates the target signal detection (CFAR detection with binary integration).

For a GPS L5 receiver, the frequency bandwidth is 20.46 MHz, and the noise level N_r in decibels is nearly -131 dB. The signal-to-noise ratio at the RF front-end output of the GPS receiver can be written as (Glennon et al., 2006):

$$SNR = P_{rec} / N_r = P_t G_r \sigma / (4\pi R_{ig}^2 N_r) \quad (2)$$

According to [2,6,7], the forward scatter RCS σ of a target depends only on the physical cross section of the target (A_{ig}) and can be calculated approximately as:

$$\sigma = 4\pi A_{ig}^2 / \lambda^2 = 4\pi(hl)^2 / \lambda^2 \quad (3)$$

In (3), A_{ig} is the target physical cross section, and the parameters h and l are geometrical dimensions of a target. In order to obtain the SNR expression at the input of a CFAR detector in FSR, we replace the parameter σ in (2) by its expression (3).

$$SNR = P_t G_r (hl)^2 / (\lambda^2 R_{ig}^2 N_r) \quad (4)$$

At the output of the Code& Tracking loops the signal-to-noise ratio is given by:

$$SNR = P_t G_r (hl)^2 G_{SP} / (\lambda^2 R_{ig}^2 N_r) \quad (5)$$

where G_{SP} is the processing gain of the cross-correlator.

3 DETECTION PROBABILITY

The signal to-noise ratio (4) could be improved by non-coherent or binary integration over M samples. In the extreme case, when, for example, the target moving in the forward scattering zone at velocity V and crosses the baseline at an angle of nearly 90° , the maximum integration time corresponding to target visibility within the main lobe of the target scattering pattern is given by:

$$T_{ig} = 2d_R^2 \lambda / (Vl) \quad (6)$$

where d_R is the distance from the receiver to the point of crossing and it can be assumed that $d_R = R_{ig}$. The number of integrated samples M can be determined from (5) as:

$$M = E[T_{ig} / T_{Q5}] \quad (7)$$

where $T_{Q5} = 20 \text{ msec}$ and $E[\cdot]$ is the integer part of the fraction in brackets.

3.1 CFAR Detection with Non-coherent Integration

In a CFAR detector, after non-coherent integration of M samples of the signal intensity at the envelope detector output, the following test statistics is formed for each sample n in the time domain:

$$q_M(n) = \sum_{k=n-M/2}^{n+M/2-1} |s(k)|^2 \quad (8)$$

The intensity in n^{th} time discrete indicates signal detection if the test statistics (7) exceeds an adaptive threshold H_n . According to [7], the decision rule for detection is:

$$\Phi_M(n) = \begin{cases} 1, & \text{if } q_M(n) \geq H_n(K) \\ 0, & \text{otherwise} \end{cases} \quad (9)$$

The parameter K in (9) is the length of the reference window used to estimate the total noise level. When the noise intensity is unknown, the detection threshold $H_n(K)$ in (9) is formed adaptively for each integrated sample $q_n(M)$ of the signal intensity at the envelope detector output. In a cell-average CFAR detector the threshold $H_n(K)$ is formed as:

$$H_n(K) = T_\alpha \cdot w_n(K) \quad (10)$$

where T_α is the scale factor, $w_n(K)$ is the average power of the total noise calculated over samples if the reference window.

$$w_n(K) = \sum_{k=1}^K |s(k)|_n^2 \quad (11)$$

The probability of false alarm p_{FA} maintained at the output of a CFAR detector can be calculated using the following expression (Behar et al., 2011):

$$P_{FA} = \sum_{n=0}^{K-1} \binom{K+n-1}{K-1} \frac{T_\alpha^n}{(1+T_\alpha)^{K+n}} \quad (12)$$

In the worst case when the signal intensity from the target independently fluctuates according to the χ^2 -law, the probability of detection at the output of a CFAR detector is evaluated as follows [7]:

For $1 \leq M \leq 2$:

$$P_D = \sum_{j=L-1}^1 \binom{2-M}{1-j} \frac{\alpha^{1-j}}{\beta^{M-j-1}} \sum_{n=0}^j \binom{K+n-1}{1} \frac{(\alpha T_\alpha)^n}{(1+\alpha T_\alpha)^{K+n}} \quad (13)$$

For $M > 2$

$$P_D = \sum_{i=0}^{M-3} \binom{M-2-i}{1} \frac{(-\alpha)^2}{\beta^{M-1-i}} \sum_{j=0}^i \binom{K+j-1}{j} \frac{T_\alpha^j}{(1+T_\alpha)^{K+j}} + \sum_{m=0}^1 \binom{M-2-m}{M-3} \frac{(-\alpha)^{1-m}}{\beta^{M-m-1}} \sum_{n=0}^m \binom{K+n-1}{n} \frac{(T_\alpha \alpha)^n}{(1+T_\alpha \alpha)^{K+n}} \quad (14)$$

The parameters α and β in (13) and (14) are evaluated as follows:

$$\alpha = 1/(1+M \cdot SNR/4) \quad \text{and} \quad \beta = 1-\alpha \quad (15)$$

The parameter SNR in (15) is the average signal-to-noise ratio evaluated by (5). The scale factor T_α used in (13) and (14) is determined as a root of the equation (12) for a fixed value of the false alarm probability P_{FA} .

3.2 CFAR Detection with Binary Integration

All decisions $\Phi(n)$ at the CFAR detector output obtained within M consequential time samples are summarized and compared with a fixed integer threshold L . The binary decision rule for target detection is:

$$\Phi_M(L) = \begin{cases} 1, & \text{if } \sum_{n=1}^M \Phi(n) \geq L \\ 0, & \text{otherwise} \end{cases} \quad (16)$$

The probability of false alarm at the binary detector output is:

$$P_{FA} = \sum_{n=L}^M \binom{M}{n} (p_{FA})^n (1-p_{FA})^{M-n} \quad (17)$$

The parameter p_{FA} in (17) is the probability of false alarm maintained at the CFAR detector output, which is calculated by (13). The probability of target

detection at the binary detector output is calculated analogically:

$$P_D = \sum_{n=L}^M \binom{M}{n} (p_D)^n (1-p_D)^{M-n} \quad (18)$$

The parameter p_D in (18) is the detection probability at the CFAR detector output calculated for $M=1$.

3.3 Probability of Target Detection

According to the block-scheme of signal processing (Fig.2), the probability of target detection can be expressed by the following expression:

$$P_{targ} = P_{acq} \cdot P_D \quad (19)$$

The parameter P_{acq} in (19) is the probability of GPS signal acquisition. For the sake of simplicity we assume that outside the geometrical shadow of the target (dead zone) this parameter is close to 1.

4 NUMERICAL RESULTS

Before we calculate the probability of target detection using the expressions (12-19) need to determine the SNR at the cross-correlator output in one period of the Q5 component of the GPS L5 signal ($T_{Q5}=20\text{msec}$) because the SNR values are used for calculating the parameters α and β in (15). The SNR at the cross-correlator output is calculated for a small target ($h=1\text{m}$ and $l=1\text{m}$) as a function of the distance to the target R_{tg} . The SNR values obtained are plotted in Figure 3. The following parameters of the GPS L5 signal are used in calculations: carrier frequency – $f_0=1176\text{MHz}$ ($\lambda=0.2551\text{m}$); frequency bandwidth – $\Delta F=20.46\text{MHz}$, the GPS L5 signal power near the Earth's surface – $P_r=-154\text{dBW}$.

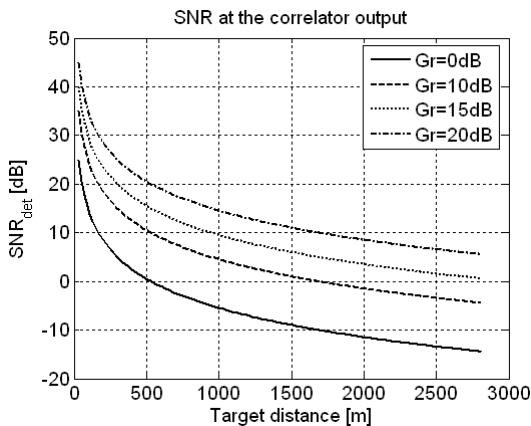


Figure 3. SNR at the correlator output within 20msec

As shown in Figure 3, the SNR is calculated for four values of the antenna gain: $G_r=[0; 10; 15; 35]$ dB.

The number of integrated samples at the correlator output and the corresponding integration time for the case when the target crosses the forward scattering zone and moving within it perpendicular to the baseline with velocity 7.5 m/s are plotted in Figure 4 depending on the distance to the target.

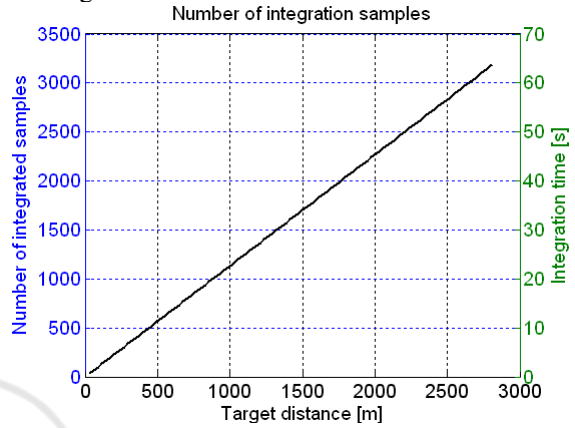


Figure 4. Number of integration samples (left) and the corresponding integration time (right)

It can be seen that the integration time can be very large and can reach to 60-70 sec for a target moving with velocity 7.5 m/s (27km/hour).

The probability of small target detection with non-coherent integration of the correlator outputs is calculated as a function of the target distance and shown in Figure 5. The probability of detection is calculated by equations (12, 13, 14) for the false alarm probability of 10^{-7} . The SNR values at the correlator output, which are used for calculation of the probability characteristics by (12, 13, and 14), are shown in Figure 3.

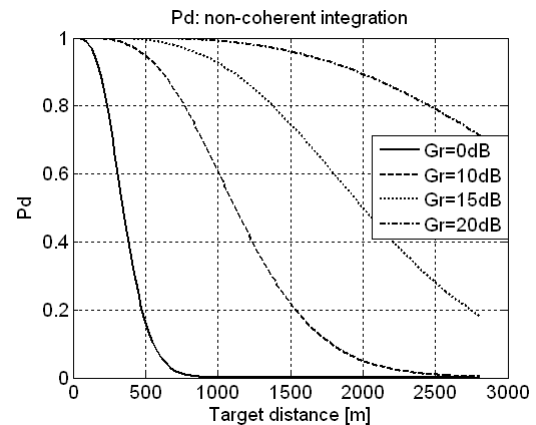


Figure 5. Probability of detection with non-coherent integration for $P_{FA}=10^{-7}$

The number of integrated samples (M) used for calculation of the probability characteristics is shown in Figure 4 (left). The size of a reference window (K) used in (13) and (14) is $K=60$.

The probability of small target detection with binary integration of the correlator outputs is calculated as a function of the target distance and shown in Figure 6. The probability of detection is calculated by equations (17, 18) for the false alarm probability of 10^{-7} . After CFAR detection at the correlator output the decision rule “ L out of M ” is used for target detection. The values of the detection probability plotted in Figure 6 are calculated for the binary threshold $L=2M/3$, where M is the number of integrated samples.

Comparing the two probabilities of detection, with non-coherent and binary integration, it can be seen that the detectability of targets strongly depends on the antenna gain that the receiver creates in the direction of the visible GPS satellite. Obviously, the greater the gain of the antenna in the direction of visible GPS satellites, so at large distances can be detected a moving target in the forward scattering area. For example, a small target that crosses the forward scattering zone can be detected with probability of 0.9 at the distance 2000m (with non-coherent integration) or 1700m (with binary integration) if the receiver antenna creates in the direction of the visible GPS satellite the gain of at least 20dB. The numerical results presented in Figure 5 and 6 also illustrate that in case of the omnidirectional antenna of the receiver ($G_r=0$ dB), small targets can be detected only at very close distances (200m-300m) regardless of the type of integration (non-coherent or binary).

Obviously, in conditions of interference, the SNR in Figure 3 must be corrected taking into account the “interference-to-noise” ratio (INR).

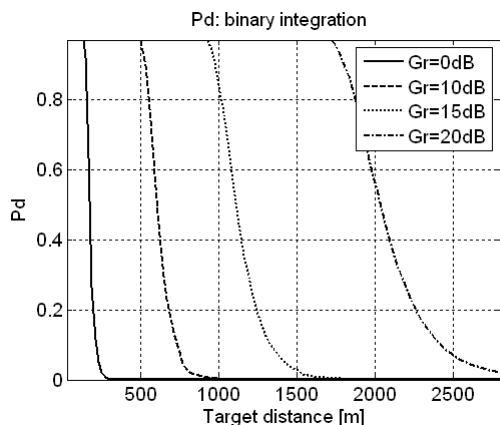


Fig.6 Probability of detection with binary integration
 $L=2M/3$ and $P_{FA}=10^{-7}$

4 CONCLUSIONS

It is shown that forward scattering radar with a non-cooperative GPS-based transmitter can be used for detection of small targets on the background of a white Gaussian noise if the receiver antenna creates in the direction of the visible GPS satellite the appropriate gain.

ACKNOWLEDGEMENTS

This work is financially supported by the Bulgarian Science Fund (projects DTK 02/28.2009).

REFERENCES

- Chernyak, V., 1999, *Fundamentals of Multisite Radar Systems*, Gordon and Breach Science Publishers.
- Cherniakov, M., Abdullah, R., Jancovic, P., Salous, M., Chapursky, V., 2006, Automatic ground target classification using forward scattering radar. In *IEE Proc. on Radar Sonar Navig.*, vol. 153, no. 5, pp. 427 – 437, October 2006.
- Koch, V., Westphal, R., 1995, New approach to a multistatic passive radar sensor for air/space defense. In *IEEE AES Systems Magazine*, pp. 24-32, November, 1995.
- Suberviola, I., Mayordome, I., Mendizabal, J., Experimental results of air target detection with GPS forward scattering radar, 2012, In *IEEE Geoscience and Remote Sensing Letters*, vol. 9, no. 1, pp.47-51, January 2012.
- Mongredien, C., Lachapele, G., Gannon, M., Testing GPS L5 acquisition and tracking algorithms using a hardware simulator, 2006. In *Proc. of ION GNSS*, Fort Worth TX, , pp. 2901-2913, September 2006.
- Behar V., Kabakchiev, Ch., Detectability of Air Target Detection using Bistatic Radar Based on GPS L5 Signals, 2011. In *Proc. IRS'2011, 12-th Intern. Radar Symp.*, Leipzig, pp. 212-217, September 2011.
- Behar, V., Kabakchiev, Ch., Rohling, H., Air Target Detection Using Navigation Receivers Based on GPS L5 Signals, 2011. In *Proc. of ION GNSS' 2011, 24th International Technical Meeting of The Satellite Division of the Institute of Navigation*, Portland OR, pp. 333-337, September 2011.
- Glennon, E., Dempster, A., Rizos, C., Feasibility of air target detection using GPS as bistatic radar, 2006. In *Journal of Global Positioning Systems*, vol. 5, no. 1-2, pp. 119-126, 2006.